Check for updates

# Multicarrier technique for 5G massive MIMO system based on CDMA and CMFB

Laila El Ghorab[1] · Ehab F. Badran[1] · Amira I. Zaki[1] · Waleed K. Badawi[1]

## Abstract

Filterbank multicarrier (FBMC) is an effective method for modulation over massive multiple-input multiple-output (MIMO) channels in the future fifth generation wireless networks. This multicarrier technique provides high spectral efficiency, and it is resilient against synchronization errors compared to the well-known orthogonal frequency division multiplexing technique. This paper introduces a new technique, that combines the Code-division multiple-access (CDMA) and cosine modulated filter banks, a specific class of FBMC, to massive MIMO communication systems. In the proposed technique, the data symbols are transmitted on different sub-bands and also, they are spread in each sub-band by CDMA code. The proposed technique reduces the interference between data symbols, which consequently improves bit-error-rate (BER) performance. Simulation results show that the overall BER performance of the proposed multicarrier transmission technique is significantly enhanced. The results obtained show that as the number of base station antennas increases, different channel distortions are averaged out, thus BER decreases (in average by $10^{-2}$) for the same signal-to-noise ratio.

**Keywords** Filterbank multicarrier (FBMC) · Massive MIMO · Code-division multiple-access (CDMA) · Cosine modulated filter banks (CMFB)

## 1 Introduction

In the future 5th generation (5G) wireless communication networks, the emergence of new data-hungry applications such as machine to machine (M2M) communication and internet of things (IOT) call for the need of larger capacity physical layer. This, in turn, has led to the development of several modulations and multicarrier techniques that are combined with massive multiple-input-multiple-output (MIMO), which is a key feature of all advanced cellular wireless systems. In multicarrier modulation systems, the overall bandwidth is divided into smaller subchannels whose equalization can be carried out independently in

✉ Waleed K. Badawi
waleedbadawi@aast.edu

1   Department of Electronics and Communication Engineering, Collage of Engineering
    and Technology, Arab Academy for Science, Technology and Maritime Transport, Alexandria,
    Egypt

a simple way. One of the most popular methods of multicarrier transmission is orthogonal frequency division multiplexing (OFDM) which attracts a lot of attention because of its ability to cope with frequency selective channels)Zaki 2019). In this system, a cyclic prefix (CP) is inserted between OFDM frames to avoid inter-symbol interference (ISI) which makes it robust to multipath fading.

The combination of OFDM and Code-division multiple-access (CDMA), which is known as multicarrier CDMA (MC-CDMA), has also received a lot of interest in wireless multimedia communications due to its excellent performance (Hara 1997) and different MC-CDMA techniques have been proposed (Sourour 1996, Kondao 1996, Vandendorpe 1995, DaSilva 1994, Sharma 2020). Despite the benefits of OFDM, there exist some drawbacks such as low spectral efficiency due to the presence of cyclic prefix, and sensitivity to time and frequency offsets caused by synchronization errors, as well as Doppler shifts. Specifically, carrier frequency offset (CFO) will cause loss of orthogonality which will lead to inter-carrier interference (ICI) that results in severe performance degradation in asynchronous multiuser applications) Zaki 2019).

An alternative method to OFDM is filter-bank multicarrier (FBMC) which was first introduced over 50 years ago by Chang (1966) and Saltzberg (1967). Compared to OFDM, FBMC is expected to provide higher bandwidth efficiency due to the absence of CP. Moreover, in the case of applying massive MIMO to FBMC systems, the linear combing of signal components smoothes channel distortion, thus, reducing the number of subcarriers significantly (Aminjavaheri 2018, Singh 2020, Hosseiny 2022, Besseghier 2022). As a result, both, the peak to average power ratio (PAPR) and the system complexity are reduced along with increasing subcarrier spacing which has the benefit of reducing the sensitivity to CFO. Another advantage of FBMC over OFDM is that it is more flexible in terms of carrier/spectral aggregation since each subcarrier band is bound to an assigned portion of the spectrum with negligible interference with other bands. Based on these benefits, FBMC is being considered as the modulation of choice for the next generation of cellular networks.

Cosine modulated filter bank (CMFB), which belongs to the class of uniform filter banks similar to FBMC/OQAM, has been widely studied in the signal processing community as well as its application to multicarrier modulation (Vaidyanathan 1993, Srivastava 2021, Masarra 2022, Besseghier 2022). In particular, it has been used for data transmission over digital subscriber line (DSL) under the name of discrete wavelet multitone (DWMT) in (Tzannes 1993) and (Sandberg 1995). Moreover, it is shown in (Farhang 2014a and b, Hosseiny 2022) that CFMB is a perfect match for massive MIMO, further studies show that performance enhancements can be achieved by using frequency spreading equalization (FSE) as introduced in (Aminjavaheri 2015). CMFB also provides a simple blind equalization method which is very beneficial in the case of pilot decontamination (Farhang-Boroujeny2003, Farhang 2014a and b).

Filterbank-based MC-CDMA (FB-MC-CDMA) schemes have been studied in single antenna systems. These systems were first proposed in (Liu 2004) and (Bianchi 2004) and further studied in (Wang 2014, Van Bolo 2017), where the performance of different FB-MC-CDMA systems in the presence of CFO is studied. Further studies show that different digital implementations of MC-CDMA can overcome the flaws of the polyphase decomposition-based fast algorithm (Gao 2006, Bian 2018, Reena raj 2021, Wang 2022).

In this paper, a new technique based on CDMA and CMFB with massive MIMO systems is proposed. In the proposed approach, the transmitted symbols are spread by a user signature code, direct-sequence CDMA (DS-CDMA), the chips belonging to different symbols are then assigned to different subcarriers by means of transmultiplexer, which allows the data symbols to be spread in each sub-band. The spread of the data

symbol in each sub-band will reduce the interference between the data symbols and hence the BER performance will be improved. To the best of the author's knowledge, the combination of the CDMA and CMFB to massive MIMO communication systems is not considered previously in the literature.

The rest of the paper is organized as follows: In Sect. 2, the proposed FB-MC-CDMA system model is described. The simulation results are shown and discussed in Sect. 3. Finally, the conclusions are presented in Sect. 4.

## 2 Proposed filterbank-based MC-CDMA system model

In this section, a new technique based on CMFB and CDMA in massive MIMO systems is introduced. Figure 1 presents the block diagram of the proposed CMFB-MC-CDMA transceiver.
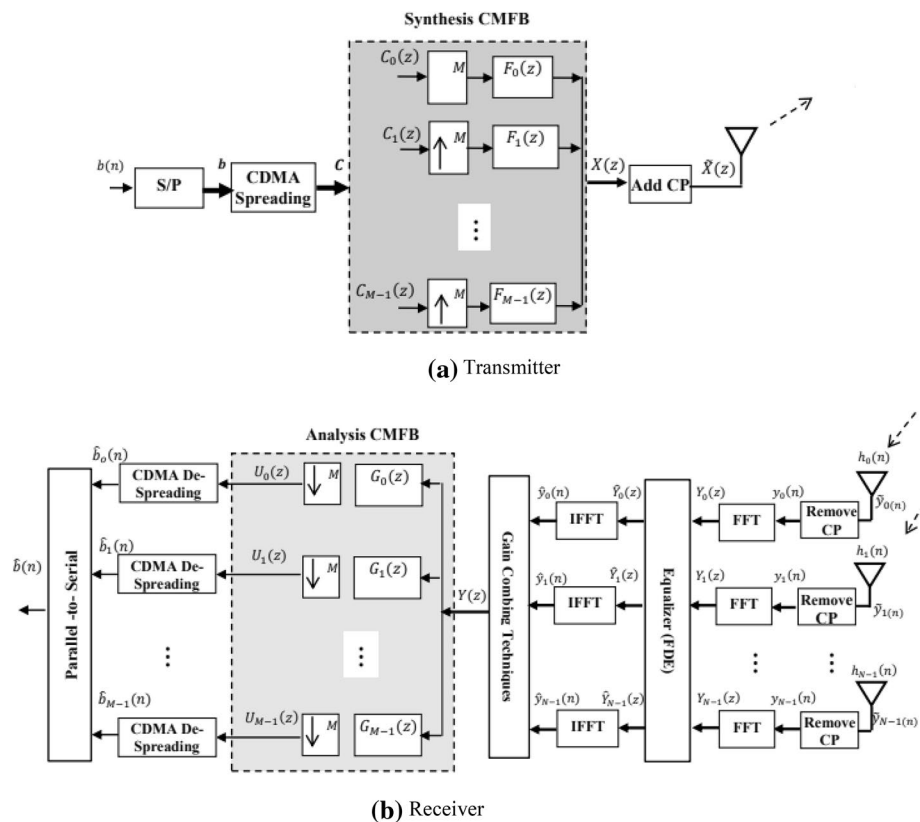


**(a)** Transmitter



**(b)** Receiver

**Fig. 1** The Proposed CMFB MC-CDMA System

## 2.1 CMFB-MC CDMA transmitter

The incoming stream of the modulated data symbols, $\{b(n)\}_{n=0}^{M-1}$, first goes through a serial-to-parallel converter (S/P) to give a vector of parallel data streams b, which is of dimensions $M \times 1$. Each symbol is then spread by a sequence $s = \begin{bmatrix} s_0 & s_1 & \cdots & s_{L-1} \end{bmatrix}^T$, the spreading sequence is unique for each user, yielding a row vector of L chips (Hara 1997),

$$C = b\ s^T = \begin{bmatrix} c_0 \\ c_1 \\ \vdots \\ c_{M-1} \end{bmatrix} = \begin{bmatrix} b(0)s_0 & b(0)s_1 & \cdots & b(0)s_{L-1} \\ b(1)s_0 & b(1)s_1 & \cdots & b(1)s_{L-1} \\ \vdots & \vdots & \ddots & \vdots \\ b(M-1)s_0 & b(M-1)s_1 & \cdots & b(M-1)s_{L-1} \end{bmatrix}, \tag{1}$$

where C represents a matrix of dimensions $M \times L$. Each row of C which contains L Chips of spread symbol b(k) are then upsampled by M. The up sampled row signal $C_k(z^M)$ with length LM is fed to a synthesis filter $F_k(z)$. Which is one of the filter bank synthesis filters? $\{F_k(z)\}_{k=0}^{M-1}$ (Vaidyanathan 1993). Hence, as shown in Fig. 1 the outputs of the synthesis filters are summed to generate the transmit signal X(z)

$$X(z) = \sum_{k=0}^{M-1} C_k(z^M) F_k(z), \tag{2}$$

which can be represented in time domain as

$$x(n) = \sum_{k=0}^{M-1} \sum_{l=0}^{N-1} f_k(n-l) c_k\left(\frac{1}{M}\right),\ n = 0,\ M,\ 2M,\ \ldots,\ M(M). \tag{3}$$

In the proposed transmitter specific synthesis filters $f_k(n)$ are selected. Theses filters are named as cosine modulated filters and represented as:

$$f_k(n) = 2p_0(n)\cos\left(\frac{\pi}{M}\left(k + \frac{1}{2}\right)\left(n - \frac{D}{2}\right) - (-1)^k \frac{\pi}{4}\right), \tag{4}$$

where, $k = 0, 1, 2, \ldots, M-1$, $p_0(n)$ is the prototype filter and D is the filter order. Finally, the cycle prefix is added to perform the transmitted signal (Vaidyanathan 1993).

## 2.2 CMFB-MC CDMA receiver

The transmit signal is sent through a single mobile terminal (MT) antenna through the channel $H_l(z)$. The received signal at the channel output after removing cycle prefix, $Y_l(z)$ is given by

$$Y_l(z) = H_l X(z) + W_l(z),\ l = 0,\ 1,\ 2,\ \ldots,\ N-1, \tag{5}$$

where $Y_l(z)$ represents the received signal at the lth base station (BS) antenna, $W_l(z)$ is the complex gaussian noise response at the lth base station, which assumed to have zero mean and variance $\sigma_{W_l}^2 I$, and $H_l$ is frequency domain equivalent matrix (channel response) between the MT and the lth BS antenna, can be generated as) Zaki 2019):

$$H_l = \mathrm{diag}\big(F\big(h_l\big)\big) \tag{6}$$

where diag($\cdot$) is represent diagonal matrix, F($\cdot$) is FFT matrix operation and $h_l = \left[ h_l(0), h_l(1) \dots h_l(L_t) \right]$ is channel impulse response of length $L_t$. At the receiver, the signals received from the N BS antennas are equalized by zero forcing equalizer (Rashich 2019) using the equalizer-weighted diagonal matrix $\Psi_l$, which can be expressed as:

$$\Psi_l = \left( H_l^* H_l \right)^{-1} H_l^*, \tag{7}$$

where $(\cdot)^*$ represent the complex conjugate transpose of matrix and $(\cdot)^{-1}$ is the inverse of the matrix. The equalizer output can be written as:

$$\hat{Y}_l(z) = \Psi_l \, Y_l(z). \tag{8}$$

The inverse Fourier transform operation is next applied to the output of the equalizer. Then, the combining process is applied using Equal gain combining (EGC) resulting in the combined signal y(n) in time domain as:

$$y(n) = \frac{1}{N} \sum_{l=0}^{N-1} \hat{y}_l(n). \tag{9}$$

The combined signal $\{y(n) \leftrightarrow Y(z)\}$ is then passed through analysis CMFB $\left\{ G_k(z) \right\}_{k=0}^{M-1}$, where each filter output is down sampled by M, to produce the received coded data symbols $\left\{ U^T \right\}_{k=0}^{M-1}$ vectors each of a dimension $1 \times L$,

$$\tilde{U}_k(z) = G_k(z) \, Y(z), \tag{10}$$

$$U_k(z) = \frac{1}{M} \sum_{l=0}^{M-1} \tilde{U}_k \left( z^{\frac{1}{M}} e^{-j \frac{2\pi l}{M}} \right), \; k = 0, \; 1, \; 2, \; \dots, \; M-1, \tag{11}$$

where $\left\{ \tilde{U}_k \right\}_{k=0}^{M-1}$ are the analysis filters outputs and $U_k$ is the kth row of the matrix U (Farhang 2014a and b).

The resulting downsampled outputs are multiplied by the corresponding chip of the spreading sequence and summed over L consecutive values to yield the received symbols $\hat{b}$,

$$\hat{b} = U d_s = \frac{1}{L} U s. \tag{12}$$

The received symbols are then passed through a parallel-to-serial converter (P/S), to generate the received stream of symbols $\hat{b}(n)$ at the input of the decision device.

However, for the analysis filters $G_k(z)$ at the receiver, complex coefficient implementation is used which gives the opportunity for blind equalization to be carried out in a simple manner as shown in (P. Vaidyanathan 1993) and (Farhang 2014a and b).

$$G_k(z) = Q_k(z) + Q_{2M-1-k}(z) \; k = 0, \; 1, \; 2, \; \dots, \; M-1, \tag{13}$$

$$Q_k(z) = d_k P_0 \left( z W_{2M}^{k+0.5} \right) \; k = 0, \; 1, \; 2, \; \dots, \; 2M-1, \tag{14}$$

$$d_k = \begin{cases} e^{j \left( \theta_k - \frac{\pi(k+0.5)D}{2M} \right)}, & k = 0, \; 1, \; 2, \; \dots, \; M-1 \\ d_{2M-1-k}^*, & k = M, \; M+1, \; \dots, \; 2M-1 \end{cases}, \tag{15}$$

where $\theta_k = (-1)^k(\pi/4)$, * denotes the conjugate operator.

In CMFB, data symbols are pulse-amplitude modulated (PAM) and transmitted through a set of vestigial side-band (VSB) subcarrier channels. Moreover, subcarrier phases are alternated between 0 and $\pi/2$ among adjacent subcarriers; this phase adjustment allows the receiver to separate the transmitted data symbols free of ISI and ICI. More details are explained in (Chang 1966) and (Farhang-Boroujeny 2010).

## 2.3 Bit error rate analysis (BER)

The BER analysis for the proposed CMFB MC-CDMA System over Rayleigh fading channels is presented. Consider the received signals in (5), by applying ZF channel equalizer as in (7) to the received signals, the equalizer output can be written as:

$$\hat{Y}_l(z) = \Psi_l Y_l(z) = X(z) + \Psi_l W_l(z) \tag{16}$$

Then the IFFT and the equal gain combiner is applied successively to get the output of the combiner as:

$$y(n) = \frac{1}{N}\sum_{l=0}^{N-1} x(n) + \Psi_l w_l(n) = x(n) + \frac{1}{N}\sum_{l=0}^{N-1}\Psi_l w_l(n). \tag{17}$$

The operations of filtering (using analysis CMFB where each filter output is down sampled), CDMA de-spreading, and parallel to serial converter are applied to get received stream of symbols $\hat{b}(n)$ using (10), (11), and (12) as (Sharma 2020):

$$\hat{b}(n) = b(n) + \eta, \tag{18}$$

where

$$\eta = d_s\, G(z) \cdot F(\ddot{w}(n)) = d_s\eta_G, \tag{19}$$

$$\ddot{w}(n) = \frac{1}{N}\sum_{l=0}^{N-1}\Psi_l w_l(n) = \frac{1}{N}\sum_{l=0}^{N-1}\check{w}_l(n). \tag{20}$$

The average of many uncorrelated noise vectors $\hat{w}_1 \sim \mathbb{CN}\left(0;\sigma_{\hat{w}_1}^2\, I\right)$ reduce the output variance to $\frac{1}{N}$ of the average of the variances of noise vectors, which can be expressed as:

$$\sigma_{\ddot{w}}^2 = E\left[\left(\frac{1}{N}\sum_{l=0}^{N-1}\check{w}_l(n)\right)\cdot\left(\frac{1}{N}\sum_{l=0}^{N-1}\check{w}_l(n)\right)^*\right], \tag{21}$$

$$\sigma_{\ddot{w}}^2 = \frac{1}{N^2}\left[\sigma_{\check{w}_1}^2\, I + \sigma_{\check{w}_1}^2\, I + \ldots + \sigma_{\check{w}_{N-1}}^2\, I\right], \quad E\left(\check{w}_i, \check{w}_j\right) = 0. \tag{22}$$

The noise vector $\check{w}_1$ is resultant of multiplication of diagonal matrix $\Psi_1$ by noise vector $w_1 \sim CN\left(0;\sigma_{w_1}^2 I\right)$. The resultant variance of $\check{w}_1$ given by:

$$\sigma_{\check{w}_1}^2 = E\left[(\Psi_1 w_1)(\Psi_1 w_1)^*\right] = E\left[(\Psi_1 w_1 w_1^* \Psi_1^*)\right] = \Psi_1\left(\sigma_{w_1}^2\right)\Psi_1^* = \sigma_{w_1}^2\,\Psi_1\Psi_1^*. \tag{23}$$

The average value of the variance in this case can be represented as:

$$\sigma^2_{\widetilde{w}_1 \Psi} = \frac{\sigma^2_{w_1}}{M + D - 1} \sum_{f=1}^{(M+D-1)} \left| \Psi_1(f, f) \right|^2 = \alpha_1 \sigma^2_{w_1}, \tag{24}$$

$$\alpha_1 = \frac{1}{M + D - 1} \sum_{f=1}^{(M+D-1)} \left| \Psi_1(f, f) \right|^2, \quad 1 = 0, \ 1, \ \dots, \ N - 1. \tag{25}$$

As, $\sigma^2_{\hat{w}_1} = \alpha_1 \sigma^2_{w_1}$ and using (22) then,

$$\sigma^2_{\tilde{w}} = \frac{1}{N^2} \left[ \alpha_0 \sigma^2_{w_0} I + \alpha_1 \sigma^2_{w_1} I + \dots + \alpha_{N-1} \sigma^2_{w_{N-1}} I \right] = \frac{1}{N^2} \sum_{l=0}^{N-1} \alpha_1 \sigma^2_{w_1}, \tag{26}$$

$$\sigma^2_{\tilde{w}} = \frac{1}{N^2} \sum_{l=0}^{N-1} \sigma^2_{\tilde{w}_1}. \tag{27}$$

Since the analysis CMFB is linear time invariant filter and the down sampling operation do not affect the noise variance, so the output noise variance of the filter can be represented as:

$$\sigma^2_{\eta_G} = \left| G(z) \right|^2 \cdot \sigma^2_{\tilde{w}}. \tag{28}$$

As the variance of η in (16) is given by $E(\eta\eta^*)$ as follows:

$$E(\eta\eta^*) = E\left( d_s \eta_G \left( d_s \eta_G \right)^* \right) = d_s E\left( \eta_G \eta_G^* \right) d_s^* = \frac{\sigma^2_{\eta_G}}{L} \tag{29}$$

Hence, using the relations (26), (28), and (29) the final resultant noise variance η in (19) can be expressed as

$$\sigma^2_\eta = \frac{\left| G(z) \right|^2}{L} \cdot \frac{1}{N^2} \sum_{l=0}^{N-1} \alpha_1 \sigma^2_{w_1}. \tag{30}$$

Considering noise vectors $w_1$ have the same variance, thus the final resultant noise variance in (30) can be rewritten as:

$$\sigma^2_\eta = \frac{\left| G(z) \right|^2}{L} \cdot \frac{\sigma^2_w}{N^2} \sum_{l=0}^{N-1} \alpha_1 \tag{31}$$

As notice that in (31) the resultant noise variance reduced by factor L due to the use of the CDMA spreading process in proposed technique compared to the conventional technique that not considered CDMA Spreading process.

## 3 Simulation results and discussion

This section presents a set of computer simulations, for the bit-error-rate (BER) performance, to verify the accuracy of the proposed model. In this section, simulations are performed for a multiuser MIMO and massive MIMO scenarios, where K mobile terminals

(MTs) communicate with a base station (BS) in a time division duplex (TDD) manner is assumed (T. Marzetta 2010). The BS is equipped with N transmit/receive antennas while each MT is equipped with a single transmit and receive antenna. The number of BS antennas is considered to be much larger than the number of users ($N \gg K$) and all users in the cell can simultaneously use all the subcarriers. Signals of different users are identified by the BS through their respective subcarrier gains between each MT antenna and the BS antennas, since the channel gain vectors for different users are statistically independent with respect to each other.

The results obtained are for a prototype filter of length equal to 4 M. The BER performance is tested in multipath Rayleigh fading channels and for a sample set of channel responses generated according to the SUI-4 channel model proposed by the IEEE802.16 broadband wireless access group (IEEE802.16 2001).

Furthermore, BER is also obtained for SISO, MIMO and massive MIMO systems in single user and multiuser scenarios for comparison. Additionally, in the multiuser scenario, BER is presented for both cases when MT is equipped with single and 2 transmit/receive antennas. Finally, the effect of increasing number of subcarriers is presented.

### 3.1 CMFB in SISO systems

By considering the single user scenario, the response of CMFB in single tap Rayleigh fading channel, for both BPSK and 4-PAM, is presented in Fig. 2 for number of subcarriers $M = 64$. As shown in the Fig. 2, a BER of $10^{-4}$ is achieved at SNR $= 17.5$ dB for 4-PAM modulation where in the case of BPSK, the same BER is achieved at SNR $= 10.8$ dB. Furthermore, Fig. 3 shows the BER in case of 3-tap multipath Rayleigh fading channel. The performance of both BPSK and 4-PAM degrades significantly in such channels. As noticed from Fig. 3, for 4-PAM modulation a BER of $2 \times 10^{-2}$ is achieved at SNR $= 19$ dB while for BPSK modulation the same BER is achieved at SNR $= 12.5$ dB. Thus, it is concluded that BPSK outperforms the 4-PAM modulation by 6.5 dB, however, this is at the expense of data rate.



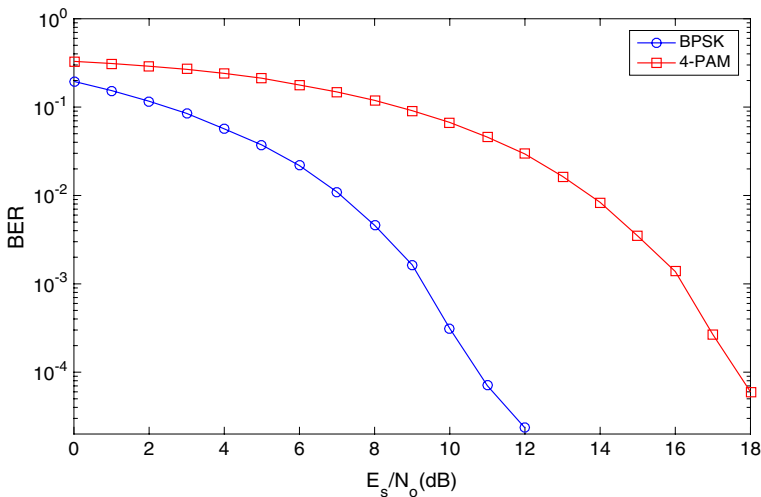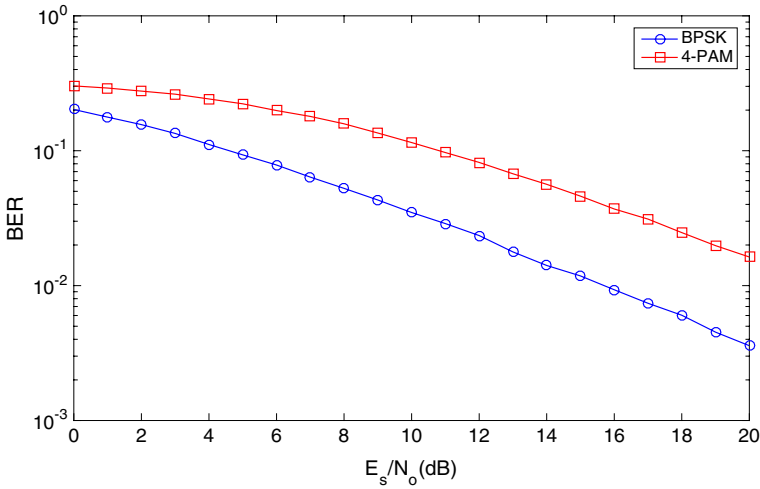**Fig. 2** BER of CMFB versus $E_s/N_0$ for $M = 64$ and SISO in single tap Rayleigh fading channel

**Fig. 3** BER of CMFB versus $E_s/N_0$ for M = 64 and SISO in 3-tap Rayleigh fading channel
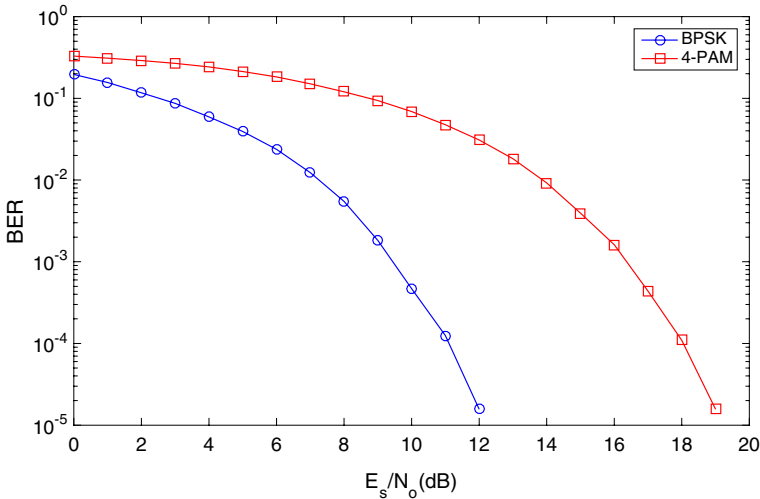


**Fig. 4** BER of CMFB versus $E_s/N_0$ for M = 64 and SISO in SUI-4 channel

Next, the performance of CMFB system is considered in the SUI-4 channel model defined by the IEEE802.16 broadband wireless access group and the results are presented in Fig. 4. As shown from Fig. 4, the BER performance degrades slightly, compared to the performance in single tap Rayleigh fading channel, for both 4-PAM and BPSK to give a BER of $10^{-4}$ at SNR = 18 dB and at SNR = 11 dB respectively.

## 3.2 CMFB in MIMO and massive MIMO systems

In a single user scenario, the effect of increasing the number of antennas at the receiver on the BER is evaluated and presented for 4-PAM modulation and M = 64 in Fig. 5. As depicted in Fig. 5, a BER of $10^{-4}$ is achieved at SNR = 11.5, 7.5 and 5.5 dB for 4, 10 and 16 antennas respectively, instead of 17.5 dB when compared to a SISO system with the same parameters for single tap Rayleigh fading channel. As highlighted by these results, distortions due to multipath fading channel are averaged out as the number of antennas increases and the BER is improved. For instance, the SNR is improved by 6, 10 and 12 dB for N = 4, 10 and 16 respectively at BER = $10^{-4}$. It is worth mentioning that when the number of antennas is larger than 10 the systems is considered to be a massive MIMO system (Björnson, 2016).

Figure 6 illustrates the effect of 3-tap Rayleigh fading channel on the CMFB system in the presence of a different number of receive antennas N. As noticed from Fig. 6, the SNR is improved from 17 to 12 dB for BER = $10^{-2}$ if the number of receive antennas is increased from N = 4 to N = 16. Moreover, by comparing these results to SISO systems it can be shown that the SNR is improved by 5, 8.5 and 10 dB for N = 4, 10 and 16 respectively. Additionally, the BER performance of the practical SUI-4 channel model is given in Fig. 7. A BER of $10^{-4}$ is achieved at SNR = 12, 8 and 6 dB for N = 4, 10 and 16 respectively. These results show an enhancement of 6, 10 and 12 dB for N = 4, 10 and 16 antennas successively compared to the results of single antennas systems obtained in Fig. 4.

## 3.3 The proposed CMFB-MC-CDMA in massive MIMO channels for the single user scenario

This section presents the simulation results of the proposed system for a single user scenario, where CDMA is applied to the CMFB system in the presence of the massive MIMO system. Figure 8 illustrates the enhancement in performance, when using the proposed
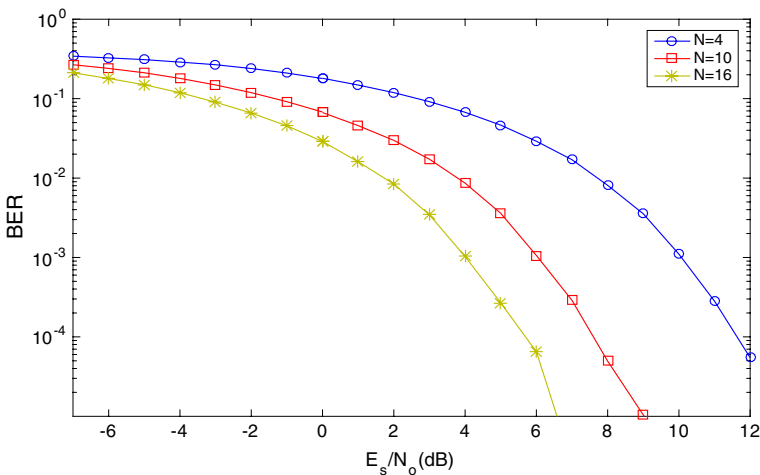


**Fig. 5** BER of CMFB versus $E_s/N_0$ for M = 64 subcarriers for different number of receive antennas N for single user scenario in single tap Rayleigh fading channel
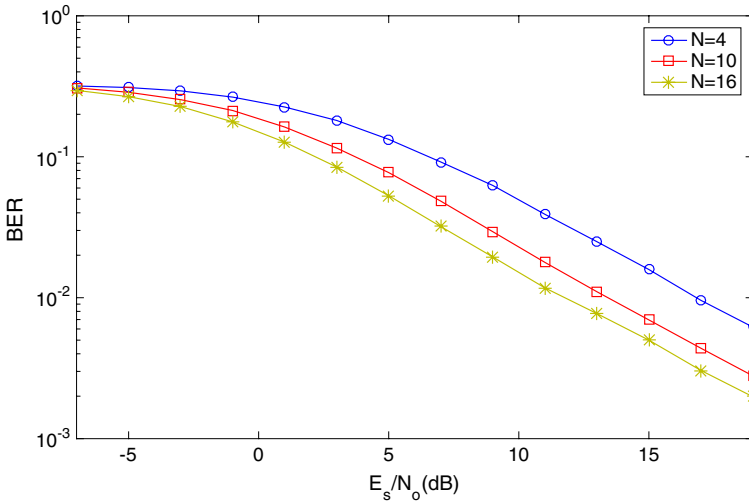
**Fig. 6** BER of CMFB versus $E_s/N_0$ for M = 64 subcarriers for different number of receive antennas N for single user scenario in 3-tap Rayleigh fading channel
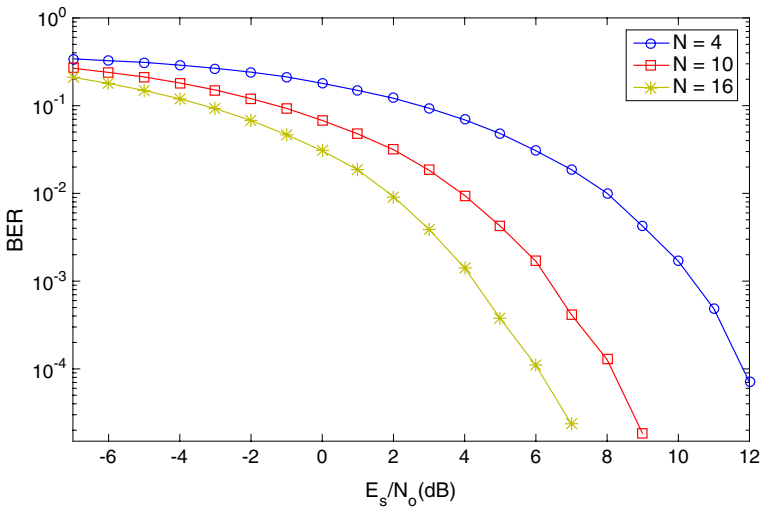


**Fig. 7** BER of CMFB versus $E_s/N_0$ for M = 64 subcarriers for different number of receive antennas N for single user scenario in the SUI-4 channel

systems, compared to the conventional CMFB system. Due to the spreading of each user signal in each sub-band, a BER of $10^{-4}$ is achieved at SNR = − 1.5 dB when CDMA is combined with CMFB while in the case when CDMA is not used the same BER is achieved at SNR = 7.5 dB. As illustrated in Fig. 8, the proposed system further improves the SNR by 9 dB for a single tap Rayleigh fading channel.

Figure 9 presents the BER performance of the proposed system and the conventional CMFB system in a 3-taps Rayleigh fading channel for N = 16 antennas. As shown in
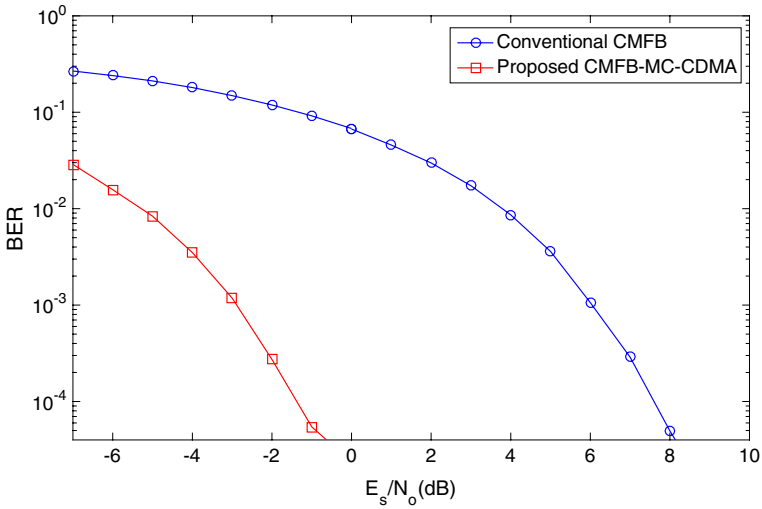
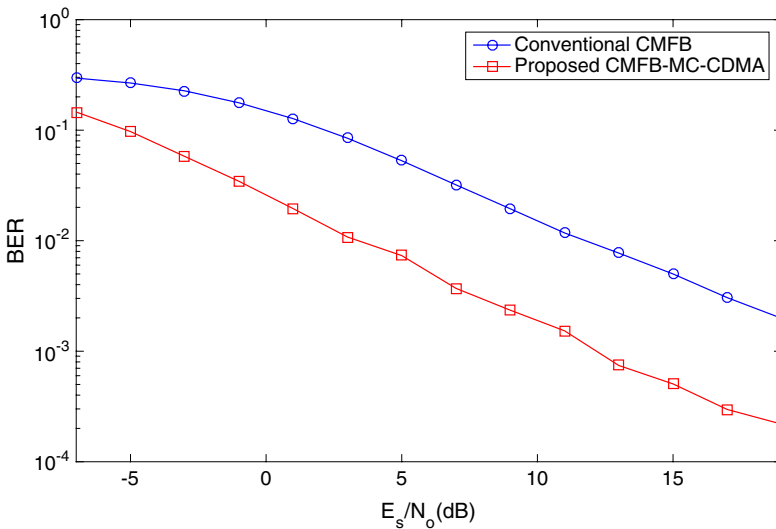**Fig. 8** BER comparison between the conventional CMFB system and the proposed CMFB-MC-CDMA for N = 10 and M = 64 in single tap Rayleigh channel

Fig. 9, the SNR needed to achieve BER = $10^{-2}$ is enhanced from 12 dB for the conventional CMFB system to 3 dB when using the proposed CMFB-MC-CDMA system, hence, introducing an overall enhancement of 9 dB. It can also be noticed from Fig. 9 that the BER reaches an acceptable value of $2 \times 10^{-4}$ at SNR = 19 dB when the proposed CMFB-MC-CDMA system is used as opposed to the conventional CMFB system in massive MIMO channels. Furthermore, the enhancement in performance achieved by the proposed



**Fig. 9** BER comparison between the conventional CMFB system and the proposed CMFB-MC-CDMA for N = 16 and M = 64 in 3-tap Rayleigh fading channel

system in the SUI-4 channel model is shown in Fig. 10. Results show that a BER of $10^{-4}$ is achieved at SNR = 8 dB for the conventional system while for the proposed system the BER of $10^{-4}$ is achieved at SNR = − 1 dB, thus, further improving the performance by 9 dB.

Since the results of SUI-4 channel model are very close to the results of a single tap Rayleigh fading channel, in the following analysis the focus will be only on one of these two models. That is, in the following section discussing the results of the proposed CMFB-MC-CDMA system in multiuser scenarios, only two channel models will be considered.

### 3.4 The proposed CMFB-MC-CDMA in massive MIMO channels for the multiuser scenario

Next, a multiuser scenario for K = 8 users is considered where the number of subcarriers M = 64 and simulations are repeated for different number of antennas N. Figure 11 illustrates the BER performance of the proposed system for different number of antennas N (N = 4,10 MIMO system and N = 16, 50 and 100 Massive MIMO system) in a single tap Rayleigh fading channel. As shown in Fig. 11, the SNR is improved by 6 dB for BER = $10^{-4}$ by increasing the number of BS antennas from 4 to 16. Comparing the results of Fig. 11 to that of Fig. 5 (single user case), it is noticed that the multiuser scenario with the proposed system gives the same results when compared to a single user scenario of the conventional CMFB system. Moreover, the effect of massive MIMO, where N ≫ K, on the proposed system model is also addressed in Fig. 11. It can be shown from Fig. 11 that a BER = $10^{-4}$ is achieved at SNR = 0.5 dB when the number of antennas is equal to 50 and the same BER is achieved at SNR = − 2.5 dB when the number of BS antennas is equal to 100. Therefore, it can be concluded that, for massive multiuser MIMO systems, the received signal can be received with power equal to or less than the noise power which increases the security of data reception.
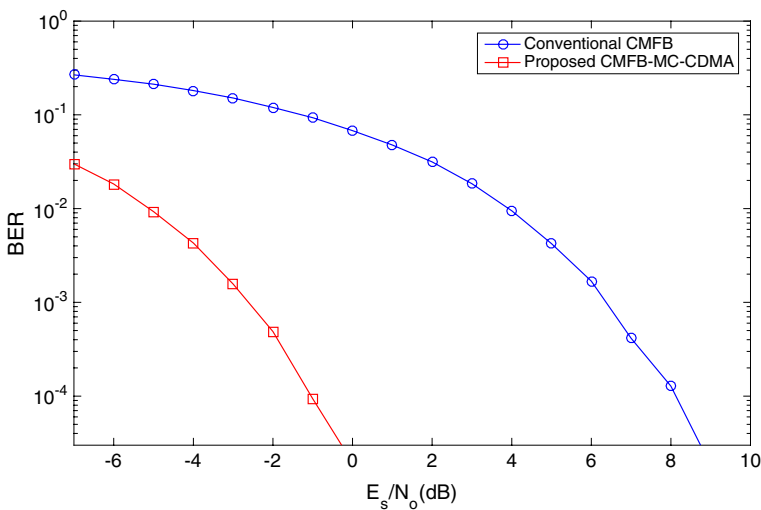


**Fig. 10** BER comparison between the conventional CMFB system and the proposed CMFB-MC-CDMA for N = 10 and M = 64 in SUI-4 channel
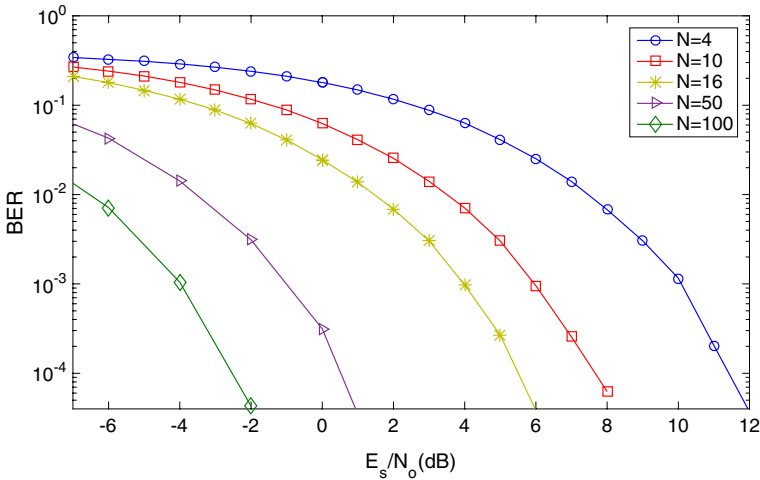
**Fig. 11** BER of CMFB-MC-CDMA versus $E_s/N_0$ for M = 64 subcarriers, K = 8 users for different number of receive antennas N in a single tap Rayleigh channel

Figure 12 shows the same multiuser scenario in 3-tap Rayleigh fading channel. At BER = $10^{-2}$ the SNR is improved from 17 to 12 dB when the number of receive antennas at the BS is increased from 4 to 16. Also, by comparing the results of Fig. 12 to that of Fig. 6 (single user case), it is noticed that the multiuser scenario with the proposed CMFB-MC-CDMA again gives the same results when compared to single user scenario of the conventional CMFB system, thus, confirming the fact that the proposed system model in the case of multiuser offers significant performance enhancement in 3-tap Rayleigh fading channel as well as the single tap channel. Additionally, when the number of receive antennas is increased to 50 and 100 as shown in Fig. 12, a BER of $10^{-2}$ is achieved at SNR = 7
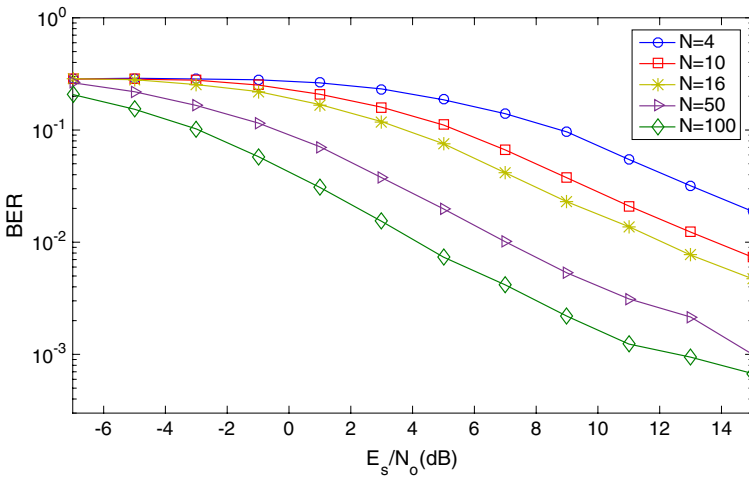


**Fig. 12** BER of CMFB-MC-CDMA versus $E_s/N_0$ for M = 64 subcarriers, K = 8 users for different number of receive antennas N in 3-tap Rayleigh channel

and 4 dB for respectively. Furthermore, Fig. 12 shows that an acceptable BER of $10^{-3}$ is achieved at SNR = 13 dB for N = 100 antennas for 3-tap Rayleigh fading channel.

Furthermore, the effect of having an MT equipped with 2 transmit antennas on the proposed CMFB-MC-CDMA system is considered in Fig. 13. The figure shows the BER performance in the case of single tap Rayleigh fading channel, where the number of receive antennas at the BS N = 16, the number of subcarriers is equal to 64 and K = 8 users. As observed from Fig. 13, having 2 transmit antennas enhances the performance by 3 dB. For instance, the SNR required to achieve BER = $10^{-4}$ is 5.5 dB when the MT has only 1 transmit antenna, while the SNR needed to achieve the same BER is 2.5 dB when the number of transmit antennas is increased to 2.

In Fig. 14, the same multiuser setup is considered for a 3-tap Rayleigh fading channel and the BER performance is evaluated. As shown in Fig. 14, the enhancement in SNR as a result of increasing the number of transmit antennas at the MT to 2 is also 3 dB for BER = $10^{-2}$. Moreover, when the number of transmit antennas is increased to 2, a BER of $10^{-3}$ is achieved at SNR = 18 dB. Although increasing the number of transmit antennas at the MT improves the performance, MTs are usually constrained by their size and cost, hence increasing the number of antennas at the MT is not an easy task since it will have an effect on the size and cost of the MT. Consequently, the rest of the simulations focus on the case where the mobile terminal is equipped with only 1 transmit antenna.

Finally, the effect of using a different number of subcarriers M on the proposed CMFB-MC-CDMA system, for the case of K = 8 users and N = 50 antennas, in both SUI-4 channel model and 3-tap Rayleigh fading channel is illustrated in Fig. 15 and Fig. 16 respectively. As shown in Fig. 16, for a BER of $10^{-4}$, the enhancement in SNR is approximately 0.5 dB when the number of subcarriers is increased to 64 instead of 8. Moreover, Fig. 16 shows that for the same proposed system in a 3-tap Rayleigh fading channel, increasing the number of subcarriers from 8 to 64 introduces an enhancement of 0.4 dB. Therefore, it can be concluded that increasing the number of subcarriers will slightly enhance the performance at the cost of increasing the system complexity and
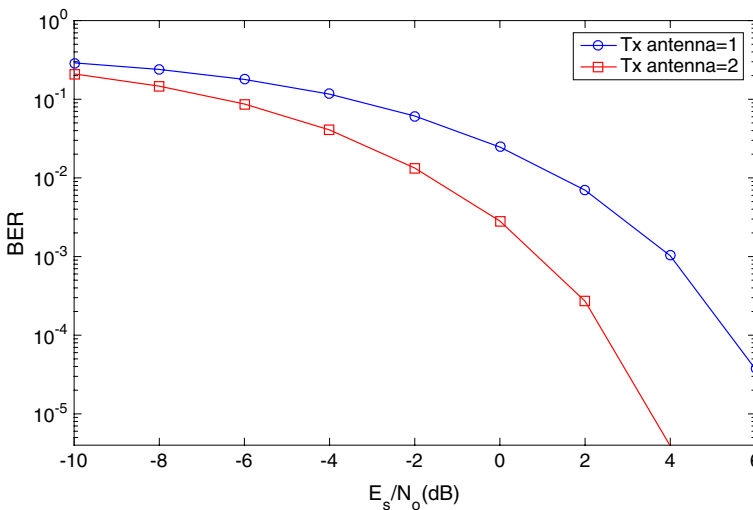


**Fig. 13** BER of CMFB-MC-CDMA versus $E_s/N_0$ for M = 64, K = 8, N = 16 with different number of transmit antennas in single tap Rayleigh channel
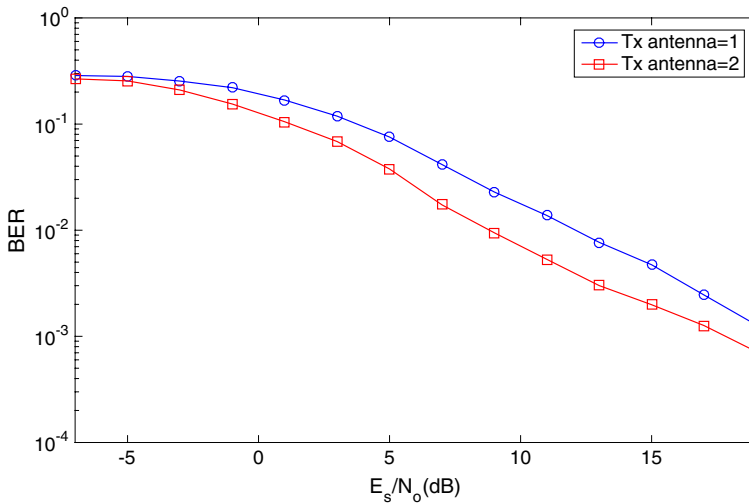
**Fig. 14** BER of CMFB-MC-CDMA versus $E_s/N_0$ for M = 64, K = 8, N = 16 with different number of transmit antennas in 3-tap Rayleigh channel
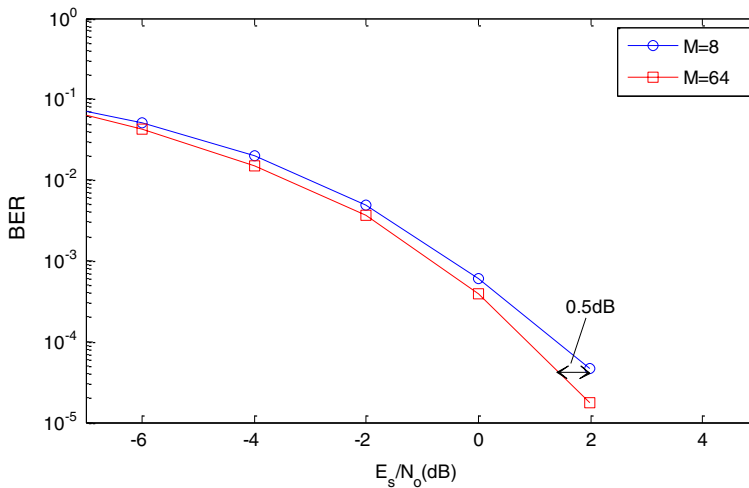


**Fig. 15** Massive MIMO CMFB-MC-CDMA system for N = 50, K = 8 and different number of subcarriers in SUI-4 channel

delay significantly. Consequently, one may significantly reduce the number of subcarriers in a MIMO CMFB-MC-CDMA system. Based on the results presented in this paper, it can be clearly shown that proposed CMFB-MC-CDMA with massive MIMO has a significant effect on enhancing the system performance.
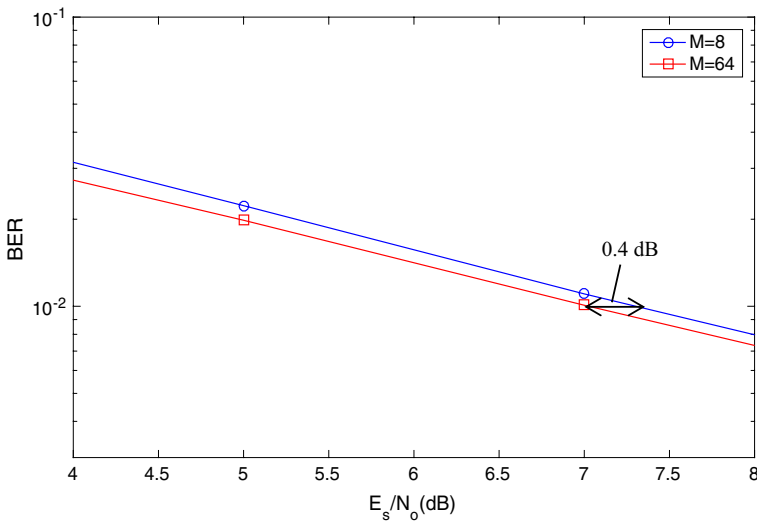
**Fig. 16** Massive MIMO CMFB-MC-CDMA system for N = 50, K = 8 and different number of subcarriers M in 3-tap Rayleigh fading channel

## 4 Conclusion

In this paper, a new CMFB-MC-CDMA massive MIMO system is introduced to improve the BER performance. For single user scenario, BER performance was studied for SISO, MIMO, and massive MIMO systems. Simulation results showed that the SNR was improved by 10 dB at BER $= 2 \times 10^{-2}$ in the case of 3-tap Rayleigh fading channel when massive MIMO for N = 16 was used compared to SISO systems. Additionally, in the SUI-4 channel model, the SNR in the case of massive MIMO for N = 16 was enhanced by 12 dB at BER $= 10^{-4}$ compared to the BER performance of SISO. Simulation results also showed that the SNR was further improved by 9 dB when the proposed system is used in a single tap Rayleigh fading channel at BER equal to $10^{-4}$ for N = 10 antennas. Moreover, for 3-tap Rayleigh fading channel, the enhancement in SNR after applying the proposed system was 8 dB for N = 10 and 9 dB for N = 16 at BER $= 10^{-2}$ when compared the conventional one.

Also, the multiuser scenario was investigated for the proposed CMFB-MC-CDMA system for 8 users. Results showed that for a BER of $10^{-2}$, the SNR was enhanced by 5 and 8 dB for $N = 50$ and 100 respectively, compared to the case where $N = 16$ in a 3-taps Rayleigh fading channel. Additionally, in a single tap Rayleigh fading channel and the SUI-4 channel, results showed that when the number of antennas was greatly increased, the power needed to receive the signal to achieve BER $= 10^{-4}$ was significantly reduced to a value that is equal to the noise power for $N = 50$. Finally, it was shown that increasing the number of subcarriers from 8 to 64 in the presence of massive MIMO system introduces only 0.5 dB improvement in SNR, thus, a smaller number of subcarriers could be used for both 3-tap Rayleigh fading channel and SUI-4 channel model. Accordingly, the system complexity and latency could be reduced. The results presented in this paper show that CMFB-MC-CDMA is a promising alternative to OFDM based MC-CDMA systems in the future 5G networks.

**Data availability** The data used and/or analyzed during the current study are available from the corresponding author on reasonable request.

## Declarations

**Conflict of interest** The authors declare that they have no competing interests and no conflict of interest.

**Ethical approval** Not Applicable.

## References

Aminjavaheri, A., Farhang, A., Farhang-Boroujeny, B.: Filter bank multicarrier in massive MIMO: analysis and channel equalization. IEEE Trans. Signal Process. **66**(15), 3987–4000 (2018)

Aminjavaheri, A., Farhang, A., Marchetti, N., Doyle, L.E., Farhang-Boroujeny, B.: Frequency spreading equalization in multicarrier massive MIMO. In: IEEE international conference on communication workshop (ICCW), pp. 1292–1297 (2015)

Besseghier, M., Djebbar, A.B., Kofidis, E.: Joint CFO and highly frequency selective channel estimation in FBMC/OQAM systems. Digit. Signal Process. **128**, 103629 (2022)

Bian, X., Tang, J., Wang, H., Li, M., Song, R.: An uplink transmission scheme for pattern division multiple access based on DFT spread generalized multi-carrier modulation. IEEE Access **6**, 34135–34148 (2018). https://doi.org/10.1109/ACCESS.2018.2850146

Bianchi, T., Argenti, F.: Analysis of the effects of carrier frequency offset on filterbank-based MC-CDMA. Glob. Telecommun. Conf. GLOBECOM 04 **4**, 2520–2524 (2004)

Björnson, E., Larsson, E.G., Marzetta, T.L.: Massive MIMO: ten myths and one critical question. IEEE Commun. Mag. **54**(2), 114–123 (2016)

Chang, R.: High-speed multichannel data transmission with bandlimited orthogonal signals. Bell Sys. Tech. J. **45**, 1775–1796 (1966)

DaSilva, V.M., Sousa, E.: Multicarrier orthogonal CDMA signalsfor quasi-synchronous communication systems. IEEE J. Sel. Areas Commun. **12**(5), 842–852 (1994)

Farhang, A., Aminjavaheri, A., Marchetti, N., Doyle, L.E., Farhang-Boroujeny, B.: Pilot decontamination in cmt-based massive mimo networks. In: Wireless communications systems (ISWCS), 2014a 11th international symposium on. IEEE, pp. 589–593 (2014a)

Farhang, A., Marchetti, N., Doyle, L., Farhang-Boroujeny, B.: Filterbank multicarrier for massive MIMO. In: Proceedings of IEEE VTC-Fall 2014b, [online] (2014b). Available: arXiv: 1402.5881

Farhang-Boroujeny, B.: Multicarrier modulation with blind detection capability using cosine modulated filter banks. IEEE Trans. Commun. **51**(12), 2057–2070 (2003)

Farhang-Boroujeny, B., George Yuen, C.: Cosine modulated and offset QAM filter bank multicarrier techniques: a continuous-time prospect. EURASIP J. Appl. Signal Process. **2010**, 16 (2010)

Gao, X., et al.: An efficient digital implementation of multicarrier CDMA system based on generalized DFT filter banks. IEEE J. Sel. Areas Commun. **24**(6), 1189–1198 (2006)

Hara, S., Prasad, R.: Overview of multicarrier CDMA. IEEE Trans. Commun. Mag. **35**, 126–133 (1997)

Hosseiny, H., Farhang, A., Farhang-Boroujeny, B.: Downlink precoding for FBMC-based massive MIMO with imperfect channel reciprocity. In: ICC 2022—IEEE international conference on communications, pp. 1324–1329 (2022). https://doi.org/10.1109/ICC45855.2022.9839271

IEEE802.16 Broadband wireless access working group, channel models for fixed wireless applications (2001)

Kondao, S., Milstein, L.B.: Performance of multicarrier DS-CDMA systems. IEEE Trans. Commun. **44**, 238–246 (1996)

Liu, M., Liu, W.-D., Sun, D.-Q., Li, R.-X., Yang, T.-X.: A MC-CDMA system based on CMFB. In: Proceedings of IEEE International Conference on Control Applications, Taipei, Taiwan, pp. 45–50 (2004)

Marzetta, T.: Noncooperative cellular wireless with unlimited number of base station antennas. IEEE Trans. Wirel. Commun. **9**(11), 3590–3600 (2010)

Masarra, M., Hassan, K., Zwingelstein, M., Dayoub, I.: FBMC-OQAM for frequency-selective mmWave hybrid MIMO systems. In: 2022 IEEE wireless communications and networking conference (WCNC), pp. 1593–1598 (2022). https://doi.org/10.1109/WCNC51071.2022.9771667

Rashich, A., Gorbunov, S.: ZF equalizer and trellis demodulator receiver for SEFDM in fading channels. In: 2019 26th international conference on telecommunications (ICT), pp. 300–303 (2019). https://doi.org/10.1109/ICT.2019.8798843

Reena Raj, T., Sakthidasan Sankaran, K., Nagarajan, V.: Chaotic sequence-based MC-CDMA for 5G. Concurr. Comput. Pract. Exp. **33**(4), e4992 (2021e)

Saltzberg, B.: Performance of an efficient parallel data transmission system. IEEE Trans. Commun. Technol. **15**(6), 805–811 (1967)

Sandberg, S., Tzannes, M.: Overlapped discrete multitone modulation for high-speed copper wire communications. IEEE J. Sel. Areas Commun. **13**(9), 1571–1585 (1995)

Sharma, S., Melvasalo, M., Koivunen, V.: Multicarrier DS-CDMA waveforms for joint radar-communication system. In: 2020 IEEE radar conference (RadarConf20), pp. 1–6 (2020). https://doi.org/10.1109/RadarConf2043947.2020.9266515

Singh, P., Mishra, H.B., Jagannatham, A.K., Vasudevan, K., Hanzo, L.: Uplink sum-rate and power scaling laws for multi-user massive MIMO-FBMC systems. IEEE Trans. Commun. **68**(1), 161–176 (2020). https://doi.org/10.1109/TCOMM.2019.2950216

Sourour, E.A., Nakagawa, M.: Performance of orthogonal multicar- rier CDMA in a multipath fading channel. IEEE Trans. Commun. **44**, 356–367 (1996)

Srivastava, S., Singh, P., Jagannatham, A.K., Karandikar, A., Hanzo, L.: Bayesian learning-based doubly-selective sparse channel estimation for millimeter wave hybrid MIMO-FBMC-OQAM systems. IEEE Trans. Commun. **69**(1), 529–543 (2021)

Tzannes, M., Tzannes, M., Resnikoff, H.: The DWMT: a multicarrier transceiver for ADSL using M-band wavelet transforms. ANSI contribution T1E1.4/93–067, (1993)

Vaidyanathan, P.: Multirate systems and filter banks. Prentice Hall, Englewood Cliffs (1993)

Vandendorpe, L.: Multitone spread spectrum multiple access communi-cations system in a multipath Rician fading channel. IEEE Trans. Veh. Technol. **44**(2), 327–337 (1995)

Van Bolo, I., Espera, T.P., Marquez, R.V., Ambatali, C.D., Bernardo, N.I.: Performance evaluation of spread spectrum-based multiple access combined with 5G filter-based multi-carrier waveforms. In: 2017 11th international conference on signal processing and communication systems (ICSPCS), pp. 1–6 (2017). https://doi.org/10.1109/ICSPCS.2017.8270475

Wang, Z., Fan, S., Rui, Y.: CDMA-FMT: A novel multiple access scheme for 5G wireless communications. In: 19th international conference on digital signal processing, pp. 898–902. Hong Kong (2014)

Wang, J., Li, D., Zhang, Z., Chen, X.: Traffic offloading and resource allocation for PDMA-based integrated satellite/terrestrial networks. In: 2022 IEEE 4th international conference on power, intelligent computing and systems (ICPICS), pp. 259–262 (2022) https://doi.org/10.1109/ICPICS55264.2022.9873721

Zaki, A.I., Hendy, A.A., Badawi, W.K., Badran, E.F.: Joint PAPR reduction and sidelobe suppression in NC-OFDM based cognitive radio using wavelet packet and SC techniques. J. Phys. Commun. **35**, 100695 (2019). https://doi.org/10.1016/j.phycom.2019.04.009

Springer